Materials and Structures (2024) 57:187
https://doi.org/10.1617/s11527-024-02462-3

ORIGINAL ARTICLE

Effects of kaolinite and montmorillonite calcined clays on the sulfate balance, early hydration, and artificial pore solution of limestone calcined clay cements (LC^3)

Micael Rubens Cardoso da Silva · Jose da Silva Andrade Neto · Brant Walkley · Ana Paula Kirchheim

Received: 4 October 2023 / Accepted: 5 September 2024

Abstract This study investigated the physicochemical effects of kaolinite (CK) and montmorillonite (CM) calcined clays on the sulfate balance, early hydration, and artificial pore solution of limestone calcined clay cement (LC^3). The effects of fineness, clay dissolution, and ion-adsorption capacity were evaluated by isothermal calorimetry, compressive strength, ICP-OES, and zeta potential within 72 h, respectively. Increasing the fineness of both calcined clays did not significantly affect the sulfate depletion kinetics or the compressive strength and the adsorption of Ca^{2+} ions onto the calcined clay's surface is not the main factor responsible for differences in sulfate demand. The higher dissolution of ions Al in CK provided an intensified and accelerated formation of ettringite that competes for the available sulfate. We demonstrate that the chemical effects have a significant impact on the sulfate balance of LC^3, revealing the lesser impact of alternative clays like montmorillonite compared to metakaolin (MK) which can minimize the problem of accelerated sulfate depletion of LC^3 mixes with MK.

Keywords Kaolinite · Montmorillonite · Calcined clays · Sulfate balance · Sulfate demand

1 Introduction

Clays are mainly composed of minerals widely available in the earth's crust, including kaolinite, montmorillonite, and illite/mica as the most abundant [1]. Kaolinite is a typical 1:1 clay mineral of the kaolin group with the chemical formula $Al_2O_3(SiO_2)_2$. Its unit cell structure consists of the tetrahedral Si and octahedral Al layers joined by bonds of oxygen atoms. Montmorillonite has an extra layer of tetrahedral Si that encompasses the octahedral Al layer; hence they are known as a 2:1 group clay mineral [2]. Also, the montmorillonite's interlayers are bonded by weak oxygen bridges and contain a lot of active sites and exchangeable cations, which allow the entrance of water molecules or cations such as Na^+, Mg^{2+} or Ca^{2+} [3]. As a 2:1 clay mineral, it exhibits isomorphic substitution, resulting in a net negative charge balanced by interlayer cations (Ca^{2+}, Na^+, or K^+)

Supplementary Information The online version contains supplementary material available at https://doi.org/10.1617/s11527-024-02462-3.

M. R. C. da Silva (✉) · J. S. Andrade Neto · A. P. Kirchheim (✉)
Department of Civil Engineering, Universidade Federal do Rio Grande do Sul, Av. Osvaldo Aranha, 99/706, Porto Alegre, RS 90035-190, Brazil
e-mail: mrcardosodasilva1@sheffield.ac.uk

A. P. Kirchheim
e-mail: anapaula.k@gmail.com

M. R. C. da Silva · B. Walkley
Department of Chemical and Biological Engineering, The University of Sheffield, Sir Robert Hadfield Building, Mappin Street, S1 3J, Sheffield, UK

Published online: 21 September 2024

coordinated to H_2O molecules in the interlayer region [2]. Therefore, montmorillonite has strong adsorption and cation exchange, shrinkage, intercalation, and swelling capacity [3, 4], contrasting significantly with kaolinite clay minerals [5].

Clay minerals can be found in different forms in nature, such as rock, soil, or clays. *In Natura,* clays usually have low or negligible chemical reactivity, limiting their application as supplementary cementitious material (SCM) by the cement industry. Thus, mechanical, chemical, or thermal processes are used to increase their reactivity. Calcination is the most common way to enhance clay reactivity, by inducing dehydroxylation and structural disorder in the clay, which provides sufficient reactivity for the calcined clay to react with products of ordinary Portland cement (OPC) hydration and reduce the environmental impact (primarily CO_2 emissions) from the cement production by high levels of clinker substitution [6].

It is known that the kaolinite clay mineral has the highest reactivity in the cement matrix among the clay minerals [7]. However, concerns about transportation distances or shortages of raw materials may encourage other clay types for produce low-carbon cements such as limestone calcined cements (LC^3) to increase CO_2 savings further. LC^3 consists of replacing ~ 50% (wt%) of clinker with limestone and calcined clays, which reduces CO_2 emissions from cement production [8]. For instance, in Denmark, bentonite (a clay-rich in montmorillonite) has become a suitable alternative to develop blended cements since kaolin reserves are locally scarce [9].

SCMs interact with blended cement mainly through their physical and chemical effects [10]. Studies with fresh pastes confirm that calcined clays increase the requirement for water and chemical admixtures in LC^3 for a specific rheological behavior, mainly due to their high fineness, specific surface area (SSA_{BET}), and mineralogical structure [11, 12]. The effects of such SCM features on the hydration of blended cements are still a matter of debate, especially related to their impact on the sulfate balance of blended cements.

Recent studies on LC^3 have indicated a faster sulfate depletion than OPC [13]. Clays are considered responsible for accelerating sulfate depletion in LC^3 cements. The mechanisms underpinning this behavior are still under discussion, but the calcined clay filler effect (fineness), ion dissolution, and possible sulfate ion adsorption on the clay surface have all been proposed as likely mechanisms affecting this [13, 14]. The complexity of these interactions is even more remarkable considering different clay minerals other than kaolinite, such as montmorillonite, which can be incorporated into the production of these blended cements such as LC^3.

The use of calcined montmorillonite (CM) in ternary cements is rarely reported. However, some efforts have been made to assess its potential use combined with metakaolin (calcined kaolinite clay, MK) in partial cement replacements [15, 16] and with limestone [17]. The synergy between both calcined clays increased portlandite ($Ca(OH)_2$;CH) consumption and compressive strength in ternary cements [15]. In addition, by increasing this amount of MK and CM, more calcium aluminosilicate hydrate (C–A)–S–H) gel pores, hydrogarnet, and strätlingite are formed at later ages [16]. Shi et al. [17] studied limestone and CM in blended cements. However, only aspects related to sulfate resistance, pozzolanic reactivity, and porosity of different calcined clays were assessed. No further attention was given to the hydration of such blended systems, especially early age aspects, such as sulfate demand.

The amount of calcium sulfate adequate to control mainly the initial reactions of the C_3S and C_3A phases is called the optimum sulfate demand. Recent studies have shown that LC^3 requires a higher amount of calcium sulfate than OPC (thus a higher sulfate demand) due to the faster sulfate consumption during the initial reactions [13, 18]. The physical and chemical effects of the calcined clays (exclusively MK) on the sulfate balance have been attributed as one of the main reasons why this occurs, and these mechanisms involved are still under discussion. Zunino and Scrivener [13] concluded that the increase of sulfate demand in blended cements mainly related to the additional surface area that impacts the total C–S–H and ettringite formation due to their competition for sulfate ions rather than the clays' chemical composition. These authors concluded that the additional alumina content provided by the calcined clays would not be mainly responsible for the need for the extra addition of calcium sulfate (gypsum) to ensure the sulfate balance of LC^3. On the other hand, other authors [11, 19] suggest that an accelerated sulfate depletion is dependent more on the kaolinite content

of the clays than on the SSA_{BET} provided by kaolinitic clays. They believe that the higher the content of calcined kaolinite, the more Al ions are available in the solution to compete for sulfate ions, leading to faster ettringite formation at early ages. According to Zunino and Scrivener [20], calcium sulfate being adsorbed to C–S–H until its depletion could be the main factor reducing the availability of gypsum in solution. Nevertheless, in a new recent study by Zunino and Scrivener [20], it was concluded that the alumina content in highly reactive SCMs like slag and metakaolin might indeed contribute to ettringite precipitation during the acceleration phase in cases of rapid dissolution. According to the authors, the impact of this phenomenon on the overall sulfate requirement remains minimal and does not exhibit a direct correlation with the quantity of alumina present in the SCMs studied by them.

The dissolution of calcined clay minerals can also impact sulfate depletion. For instance, Maier et al. [14], studying illite and kaolinite clay minerals in alkaline solutions by inductively coupled plasma optical emission spectroscopy (ICP-OES), concluded that an acceleration of sulfate depletion in blended cements is caused by alumina interactions (from C_3A and calcined clays minerals). In calcined clays, such dissolution is dependent on clay minerals and related to their SSA, reactivity and degree of dehydroxylation, according to Garg and Skibsted [21]. Using ^{29}Si and ^{27}Al magic angle spinning nuclear magnetic resonance spectroscopy (MAS NMR), they found that in kaolinite, Si and Al dissolution are 4 and 12 times larger, respectively, than in montmorillonite. ^{27}Al MAS NMR data showed highly preferential dissolution of pentahedral aluminum sites (Al^V).

The acceleration of sulfate depletion can also be influenced by adsorption of ions during cement hydration. Such arguments were pointed out by Maier et al. [14] in blended cement concerning kaolinite and illite clay minerals. The authors have proposed that the adsorption processes of SO_4^{2-} ions and/or Ca-SO_4-complexes on the surface of calcined clays impact the rapid sulfate depletion during the hydration process, according to measurement of the zeta potential of calcined clays at specific ages. Evidence for the affinity of the clay minerals for Ca^{+2} ions was previously presented by Lei and Plank [22], where kaolinite, montmorillonite, and muscovite showed increased adsorption as a function of Ca^{2+} concentration in solution. However, the calcium sulfate adsorption on the montmorillonite clay surface, such as calcium bentonite, has not yet been evaluated. Thus, the present study evaluates changes in the zeta potential of CK, CM and gypsum in artificial pore solution within 72 h.

As noted, the impact of calcined kaolinite clays on the sulfate demand of LC^3 is still under discussion and the effects of calcined montmorillonite clays on this phenomenon have never been discussed. The work aimed to verify the physicochemical mechanisms involved in the sulfate demand of LC^3 cements based on hydration and the behavior of calcined clays in artificial pore solution. Based on the hypothesis that clays of different mineralogy have different physical and chemical effects on the parameters investigated, the valorization of alternative clays to kaolin and the understanding of the behavior of these materials at early ages, can bring important insights for the industry and science in the search for wider implementation of ternary cements, such as LC^3.

2 Materials and methods

2.1 Characterization of raw materials

In this study, Portland clinker (PC), limestone (LS) and mineral gypsum (GYP), supplied by a Brazilian cement plant, were used. A natural kaolinite clay (CK) from Pantano Grande (Brazil) and commercial sodium bentonite (montmorillonite-rich clay, CM) from Buschle & Lepper S.A., were studied. Table S1, in the Supplementary Material (SM), shows the technical specification of the Na-bentonite clay provided by the sale company. A commercially available quartz powder was also used as an inert material. Figures S1 and S2, in the SM, show the X-ray diffraction (XRD) and thermogravimetric analysis/differential thermogravimetry (TGA/DTG) data for the materials used here.

The clays were prepared according to the following steps. First, both clays were dried at 100 °C. Then, the clays were sieved (2.4 mm opening sieve) and then calcined in a static furnace at 800 °C for 1 h (with a heating rate of 10 °C/min) followed by abrupt opening of the muffle at room temperature. Then, both clays were ground in a disc grinding mill to obtain two different particle size distributions (PSD),

one coarser ($d_{v,90}$ > 27.29 µm) and one finer ($d_{v,90}$ of < 27.79 µm) than the clinker.

The PSD of the materials was measured by laser granulometry in triplicate with 60 s of ultrasound/each repetition and dispersion in isopropanol or water (See SM for a description of the grinding methodology). The specific surface area of the materials was measured using the BET method (SSA_{BET}), with a heating rate of 20 °C/min with a nitrogen gas atmosphere. The chemical composition was assessed by X-ray fluorescence (XRF) in a sequential X-ray fluorescence spectrometer between 400 and 4000 cm^{-1} wavelengths. All the characterization results are presented in Table 1.

The structure of the clay(s) (minerals) used in this study are presented in Fig. 1. The reactivity of both clays (and both PSD fractions) was assessed using the protocols from the R^3 test [23], and the results are presented in Fig. 2. Both coarser clays presented similar heat release after 24 h, indicating similar reactivity. As expected, the reactivity of both clays is increased by the decrease in the PSD. However, it is interesting to note that while the heat released by the CK clay increased by 15 J/g of solid by grinding, the amount of heat released by the CM was less than 5 J/g of solid. This confirms that the PSD of the clays was not as fine as observed in other studies, justifying the low heat release [23] (Fig. 2).

Table 1 Materials characterization

Characterization	Portland clinker (PC)	Quartz powder (QP)	Coarser Calcined kaolinite clay ($CK_{coarser}$)	Finer Calcined kaolinite clay (CK_{finer})	Coarser Calcined montmorillonite clay ($CM_{coarser}$)	Finer Calcined montmorillonite clay (CM_{finer})	Lime-stone (LS)	Gypsum (GYP)
D_{v90} (µm)	27.79	13.01	37.85	25.86	39.83	26.60	37.18	34.83
D_{v50} (µm)	9.01	4.66	14.87	10.15	15.80	10.57	10.24	8.97
D_{v10} (µm)	1.61	0.89	2.86	2.39	2.63	1.89	1.44	1.85
Dvmean	12.67	6.19	18.73	12.86	19.58	13.07	15.91	14.73
Span ($\frac{D_{v90}-D_{v10}}{D_{v50}}$)	2.90	2.60	2.36	2.31	2.35	2.34	3.49	3.67
SSA_{BET} (m^2/g)	2.51	2.71	12.00	13.79	15.35	8.46	1.02	5.11
Oxides compositions by XRF (%)								
SiO_2	19.97	96.98	45.70		61.93		0.23	0.72
Al_2O_3	3.96	2.22	38.20		19.73		0.08	0.21
Fe_2O_3	3.11	–	0.65		5.02		0.05	0.11
CaO	60.43	–	0.31		1.30		55.06	33.27
MgO	7.64	–	–		3.01		0.44	0.59
SO_3	1.21	0.34	–		1.28		0.07	43.48
K_2O	1.39	0.10	0.39		0.45		0.01	0.05
P_2O_5	0.08	–	–		0.09		0.09	–
MnO	0.15	–	–		0.02		0.01	0.03
ZnO	–	0.09	–		–		–	–
SrO	0.04	–	–		0.02		0.23	0.18
Na_2O	0.20	–	–		2.92		0.05	–
TiO_2	0.20	0.06	0.13		0.51		–	0.01
ZrO_2	–	–	–		–		–	–
LOI	1.37	14.62	10.54		3.53		43.61	21.62
%Total	99.8	100	95.92		99.8		99.9	100

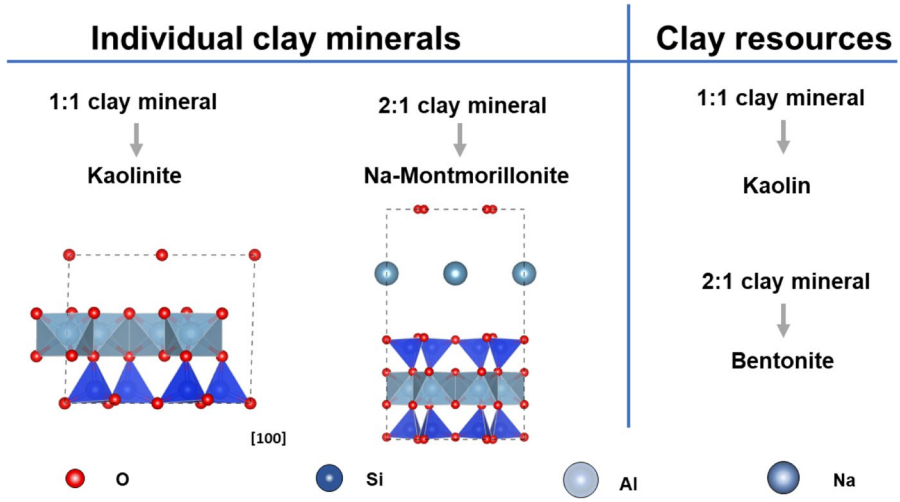

Fig. 1 Structure of the clay(s) (minerals) used in this study: kaolin (kaolinite) and bentonite (montmorillonite), using VESTA software [24]

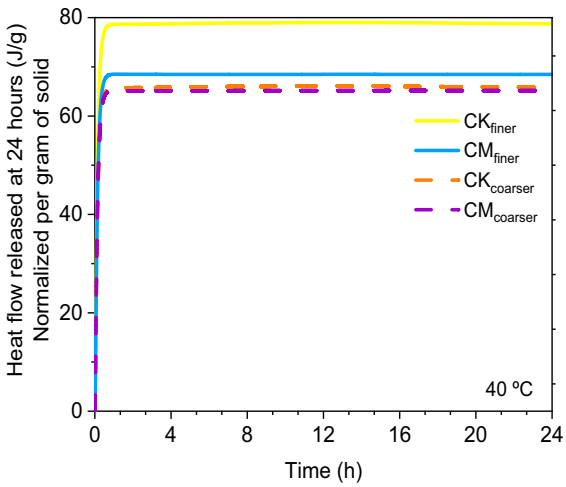

Fig. 2 Reactivity of calcined clays by R^3 test

2.2 Mix proportions

The LC^3-based blended cements were produced by following to the mix proportions suggested by Antoni et al. [8], consisting of 50% clinker, 30% calcined clay, 15% limestone, and 5% gypsum by weight (wt%). The contents of calcined clay (or quartz powder in the reference system) and limestone were kept constant across all the cements. Quartz powder was used to isolate the chemical effect of the calcined clays, as also did by Avet and Scrivener [19]. Proportions of clinker and gypsum were then adjusted based on 5 levels of SO_{3total} (2.0%, 2.5%, 3.0%, 3.5%, 4% wt%) under 4.5% SO_{3total} as required by the chemical specifications of Brazilian Portland cement [25]. SO_{3total} values were obtained by applying Eq. 1 [26], where $M_{calcium\ sulfate}$ represents the mass of calcium sulfate (gypsum), M_{cement} represents the mass of cement, $SO_{3\text{-}calcium\ sulfate}$ indicates the mass percentage of SO_3 in calcium sulfate, and $SO_{3\text{-}cement}$ denotes the mass percentage of SO_3 in the cement. The XRF results determined the SO_3 values of each material.

$$SO_3 total = \frac{M_{calcium\ sulfate}}{M_{calcium\ sulfate} + M_{cement}} \times SO_{3\ -\ calcium\ sulfate} + \frac{M_{cement}}{M_{calcium\ sulfate} + M_{cement}} \times SO_{3\ -\ cement} \quad (1)$$

Table 2 presents the mix proportions used in this study. The 15 mix were evaluated with 5 levels of $SO_{3,total}$ for the cements LC^3-QP, LC^3-CK and LC^3-CM at water:cement (w:c) ratio of 0.5. The proportion of calcined clay (or quartz powder): limestone was the same for the 3 cements (2:1). The amount of clinker and gypsum was calculated based on $SO_{3,total}$ (Eq. 1). The cements nomenclature throughout this study is as follow: *cement type-clay/quartz powder_SO$_{3total}$* (e.g., LC^3-CK_2.5%$\bar{S}$).

2.3 Experimental program

The experimental methods are organized in Fig. 3. Three hypotheses were evaluated to understand

Table 2 Mix proportions assessed in this work

Cement	PC	GYP	LS	QP	CK	CM	$SO_{3\ total}$
LC^3-QP_2.0%$\overline{S}$	52.11	2.89	15.00	30.00	–	–	2
LC^3-QP_2.5%$\overline{S}$	50.93	4.07	15.00	30.00	–	–	2.5
LC^3-QP_3.0%$\overline{S}$	49.74	5.26	15.00	30.00	–	–	3
LC^3-QP_3.5%$\overline{S}$	48.56	6.44	15.00	30.00	–	–	3.5
LC^3-QP_4.5%$\overline{S}$	47.38	7.62	15.00	30.00	-	–	4
LC^3-CK_2.0%$\overline{S}$	51.87	3.13	15.00	–	30.00	–	2
LC^3-CK_2.5%$\overline{S}$	50.68	4.32	15.00	–	30.00	–	2.5
LC^3-CK_3.0%$\overline{S}$	49.50	5.50	15.00	–	30.00	–	3
LC^3-CK_3.5%$\overline{S}$	48.32	6.68	15.00	–	30.00	–	3.5
LC^3-CK_4.0%$\overline{S}$	47.14	7.86	15.00	–	30.00	–	4
LC^3-CM_2.0%$\overline{S}$	52.78	2.22	15.00	–	–	30.00	2
LC^3-CM_2.5%$\overline{S}$	51.59	3.41	15.00	–	–	30.00	2.5
LC^3-CM_3.0%$\overline{S}$	50.41	4.59	15.00	–	–	30.00	3
LC^3-CM_3.5%$\overline{S}$	49.23	5.77	15.00	–	–	30.00	3.5
LC^3-CM_4.0%$\overline{S}$	48,04	6.96	15.00	–	–	30.00	4

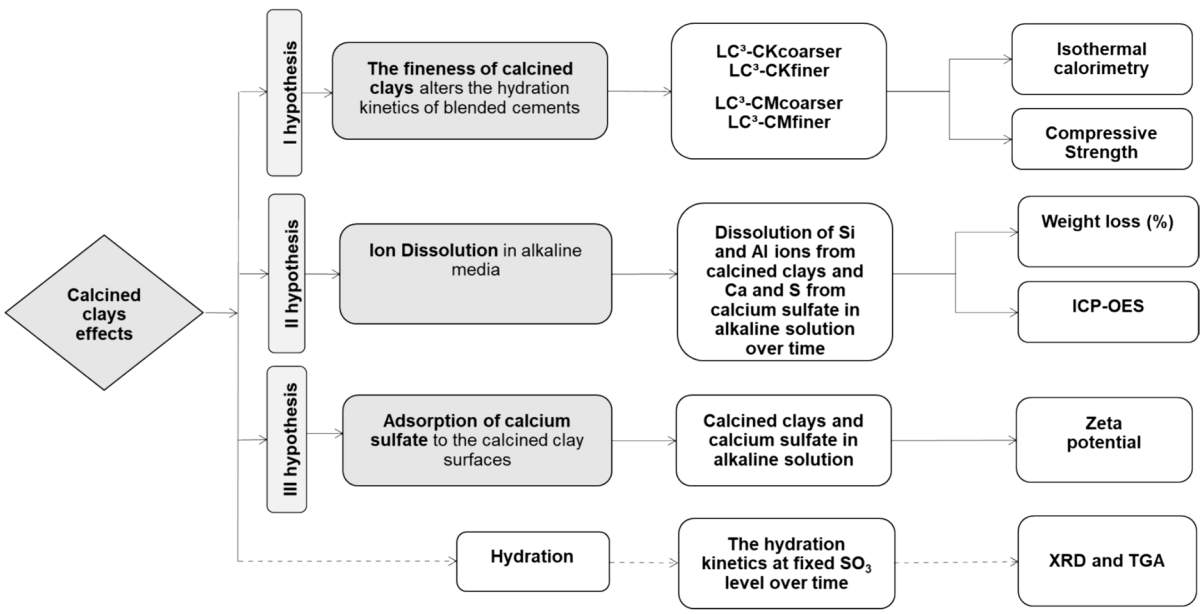

Fig. 3 Schematic representation of experimental program

better the effects of calcined clay with different mineralogy: the filler effect (fineness), dissolution under alkaline solution (as in cement hydration), and possible sulfate adsorption on the calcined clays' surface. Techniques such as isothermal calorimetry, compressive strength, ICP-OES and zeta potential measurements were used to validate each of these hypotheses, respectively. In addition, XRD and TGA data were used to assess the phase assemblage and follow the hydration in these mixes.

2.4 Test conducted

2.4.1 Mixing procedure

The mixing of LC^3 pastes were carried out in a vertical axis high shear mixer. First, 100 g of the LC^3 cement were mixed with deionized water, using a water/cement ratio equal to 0.5. The pastes were manually mixed for 30 s, and then mixed for more 70 s at 10,000 rpm mechanical mixer.

2.4.2 Isothermal calorimetry

For the isothermal calorimetry test, a TAM Air calorimeter (TA instruments) was used. Approximately 5 g of the LC^3 pastes were added into the calorimeter ampoule, and the heat flow and cumulative heat were recorded up to 72 h. Deionized water was used as reference. With this test, conclusion regarding the effect of the calcined clays fineness (CK and CM) on the hydration kinetics of the blended cements were drawn.

2.4.3 Compressive strength

For the compressive strength tests, cubic specimens (1 × 1 × 1 cm) were molded. The specimens were cured at room temperature. The compressive strength test was conducted at 3, 7 and 28 days, using a hydraulic press (model EMIC) under constant load (0.2 N/s). The compressive strength results were the mean of 5 samples for each age (in MPa).

2.4.4 TGA and XRD

To investigate the development of hydration products in cements with a fixed SO_3 content, X-ray diffraction (XRD) and thermogravimetric analysis (TGA) were carried out. After the mixing procedure used for isothermal calorimetry test, samples of paste were molded in small plastic molds, and stored at room temperature for curing. At 2, 12, 24, 48, and 72 h, the samples were ground, and their hydration stopped for solvent exchange as recommended by Snellings et al. [27]. XRD was conducted using a Rigaku Miniflex II with Bragg–Brentano geometry and a CuKα ($\lambda = 1.5418$ Å) source, operated at 30 kV and 15 mA. The samples were scanned from 5 to 70° 2θ, with a step of 0.05° 2θ and 1s per step.

TGA was performed using a METTLER TOLEDO (TGA-2) equipment, in which samples of approximately 10 mg were placed in alumina crucibles and pre-heated at 40 °C for 10 min, followed by heating up to 1000 °C at a rate of 20 °C/min. The bound water ($BW_{measured}$) was determined by measuring the weight loss (as a percentage) between 40 and 550 °C. The portlandite content ($Ca(OH)_{2,measured}$) was calculated using Eq. 2 and the results were normalized to 100 g of anhydrous cement, based on Eqs. 3–4 [28].

$$Ca(OH)_{2,measured} = WL_{Ca(OH)_2} \times \frac{m_{Ca(OH)_2}}{m_{H_2O}} \quad (2)$$

$$BW_{rescaled} = \frac{BW_{measured}}{m_{600\,^\circ C}} \quad (3)$$

$$Ca(OH)_{2,rescaled} = \frac{Ca(OH)_{2,measured}}{m_{600\,^\circ C}} \quad (4)$$

The weight loss ($WL_{Ca(OH)_2}$) attributed to the decomposition of portlandite was calculated by integrating the DTG peak located between approximately 400 and 500 °C, using the tangential method [28]. The molecular mass of portlandite (74 g/mol) was denoted as $m_{Ca(OH)_2}$, whereas m_{H_2O} (18 g/mol) represented the molecular mass of water. The weight of the sample at 600 °C (expressed as a percentage) was noted as $m_{600°C}$.

The combined water fraction (*cwf*) was subsequently computed using Eq. 5 [22], wherein $Bw_{rescaled}$ is the bound water content rescaled to 100 g of anhydrous cement and Tw represented the total water content in the mix.

$$cwf = \frac{BW_{rescaled}}{TW} \quad (5)$$

2.4.5 ICP-OES

The dissolution of the calcined clays was estimated in two different ways. The first one was using ICP-OES, where the concentration of silicon (Si) and aluminum (Al) ions from the calcined clays and calcium (Ca) and sulfur (S) from calcium sulfate were measured in

MOH solution and pH near Portland cement hydrate (~ 13.5) as described by Maier et al. [14], at 2, 12, 24, 48 and 72 h.

The mixed hydroxide solution (MOH) was based on 50 mmol/l NaOH and 300 mmol/l KOH to a pH close to 13.5 [29] at a solid calcined clays (or calcium sulfate) sample. Such alkaline solution aimed to simulate a cement pore solution pH and isolate the solubility of the calcined clays in the reaction environment as closely as possible to the real pore solution of cements hydrated. Each solution was made based on what Scherb et al. [30] suggest, where 0.25 g of the sample was eluted in 100 ml of MOH. The solution was shaken in Dubnoff water bath at 22 ± 1 °C for 72 h. The eluted sample was filtered and acidified at each test time to a pH of ~ 1 to prevent further ion dissolution. Then, 25 µL of the solution is diluted in 25 mL of milli-Q water. The solution's elements were compared with the calibration curve of each interested element. Results were measured in ppm.

2.4.6 Weight loss (%)

The solid materials retained on the filter after ICP-OES sample preparation were oven-dried to remove any free water. The gypsum was heated at 40 °C and the clays at 100 °C for 24 h. The retained material was carefully removed using a small spatula and weighed on a 0.0001 g precision balance. The difference between the "raw" material (before dissolution) and the dissolved material (after dissolution time) was used to calculate the percentage (%) of soluble and insoluble material. The % soluble expresses the reactive material that would participate in the cement reactions, in particular, Si and Al ions or Ca and S in the case of calcined clays or gypsum, respectively.

2.4.7 Zeta potential

The samples were made by mixing 1 g of material in 1L of the alkaline solution (MOH) used for ICP-OES tests, mixed at 200 rpm for 15 min. The zeta potential results were calculated from the colloidal current vibration and expressed and in mV.

3 Results

3.1 Hypothesis 1: the fineness of calcined clays alters the hydration kinetics of blended cements

Figure 4 shows the heat flow (left) and cumulative heat flow (right) of the LC^3 pastes with coarser or finer calcined clays, normalized by gram of clinker.

In general, all mixes had an induction period of approximately 2 h and a quite similar silicate heat flow peak among all mixes. The mineral additions affect this peak via a filler effect either due to the shear conditions of the particles or to the combined fineness of SCMs (calcined clays + limestone) increasing the nucleation of C_3S sites [19, 31]. Additionally, in systems with limestone, such as LC^3, there is a dominant mechanism that can still be attributed to the high affinity of Ca^{2+} to be adsorbed onto clinker surface providing an 'easy' pathway for C–S–H nucleation [31].

That increased nucleation and growth of C–S–H during cement hydration leads to two main effects on the heat flow results: the intensification of the silicate peaks and acceleration of the sulfate depletion, SD. The calcined clay fineness and the SO_3 levels slightly enhanced the first one. As shown in Table 3, in the coarser calcined clays, LC^3-$CK_{coarser}$ obtained values of silicate heat flow peaks between 4.65 and 4.88 mW/g of clinker among the SO_3 contents, while LC^3-$CM_{coarser}$ was 4.86–4.98 mW/g of clinker. In the finer calcined clays, LC^3-CK_{finer} had values from 5.08 to 4.97 mW/g of clinker while LC^3-CM_{finer} between 4.70 and 4.91 mW/g of clinker. Note that LC^3-CM_{finer} mixes had the lowest silicate heat flow. Such reduction of reactivity may be consequence of reduced SSA_{BET} due to agglomeration of particles under mechanical impact, as also observed by previous work with montmorillonite clay [32]. Nevertheless, all the peak intensities were within the range observed for LC^3-cements with different kaolinite clay contents, normalized per gram of clinker, found in the literature [19].

The second effect, the acceleration in SD, occurs when the calcium sulfate is adsorbed by the C–S–H surface up to a "depletion" point, marked by the curve that occurs just after the silicate peak [13]. Table 3 shows the position of this point occurred at different times for each cement. The coarser calcined clays had SD occurring approximately between 12 and 45 h

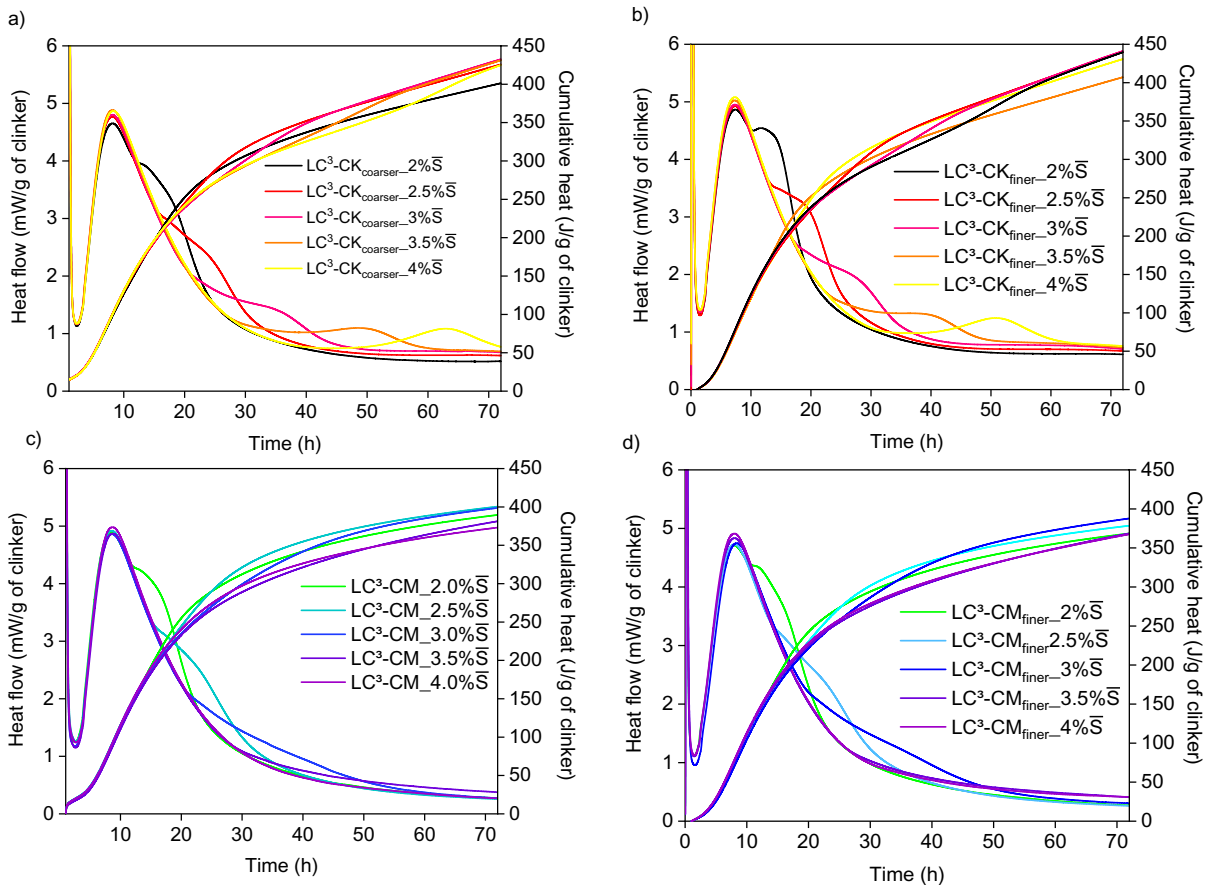

Fig. 4 Calorimetry results. **a** LC^3-CK$_{coarser}$, **b** LC^3-CK$_{finer}$, **c** LC^3-CM$_{coarser}$ and **d** LC^3-CM$_{finer}$. Heat flow (left) and cumulative flow (right) of the LC^3 cement pastes

for LC^3-CK$_{coarser}$ mixes, and between 12 h to more than 72 h in the LC^3-CM$_{coarser}$. On the other hand, increasing the fineness of both calcined clays led to an acceleration in SD. For instance, LC^3-CK$_{finer}$ had SD between 10 and 36 h, whereas LC^3-CM$_{finer}$ had intervals from 10.5 to over 72 h. Hence, the results suggested an effect of the calcined clay fineness on the hydration kinetics of LC^3 (in terms of C–S–H nucleation), as indicated by the accelerated SD from early age.

The fineness of the constituent materials of LC^3**,** especially calcined clays, must be controlled during grinding to reduce high sulfate demand or rheology problems. This is a problem when co-milling in large ball mills involving materials of different hardness is performed, such as clinker and gypsum. In the context of this complex milling procedure, an excess grinding of calcined clays can lead to undersulfated LC^3 systems. This occurred for Py [33] who discussed high efficiency grinding in disc mills. Consequently, those systems with high-fine clays blended with limestone and Portland cement were undersulfated with poor rheology. When this happens, it is necessary to use an even larger amount of gypsum in the cement, which can lead to reduced mechanical strength caused by the reduced clinker content at high levels. Also, adding large amounts of gypsum is not the best solution. As previously mentioned, it also produces longer and delayed aluminate peaks, which often does not ensure adequate cement hydration.

The SD also marks the onset of the second heat flow peak (aluminate). In this peak, there is a new and fast dissolution of the C_3A while sulfate ions are desorbed from the C–S–H, leading to a second and intensified ettringite precipitation [13, 18]. Zunino and Scrivener [13] demonstrate a strong correlation

Table 3 Additional isothermal calorimetry data

Cement	1st peak (dissolution of C_3S, precipitation of C–S–H)		2nd peak (dissolution of C_3A and precipitation of ettringite)	
	Heat flow (mW/g of clinker)*	Position (h)*	Heat flow (mW/g of clinker)s*	Position (h)*
LC^3-$CK_{coarser}$_2%$\overline{S}$	4.65	8.23	3.88	12.14
LC^3-CK_{finer}_2%$\overline{S}$	4.87	7.43	4.54	10.38
LC^3-$CK_{coarser}$_2.5%$\overline{S}$	4.77	8.11	2.43	16.14
LC^3-CK_{finer}_2.5%$\overline{S}$	4.92	7.42	3.21	13.63
LC^3-$CK_{coarser}$_3%$\overline{S}$	4.80	8.18	1.40	21.31
LC^3-CK_{finer}_3%$\overline{S}$	4.95	7.34	1.88	17.15
LC^3-$CK_{coarser}$_3.5%$\overline{S}$	4.88	8.14	1.09	37.87
LC^3-CK_{finer}_3.5%$\overline{S}$	5.01	7.33	1.30	22.37
LC^3-$CK_{coarser}$_4%$\overline{S}$	4.87	8.33	*	45.04
LC^3-CK_{finer}_4%$\overline{S}$	5.08	7.31	1.24	36.08
LC^3-$CM_{coarser}$_2%$\overline{S}$	4.89	8.47	4.25	11.97
LC^3-CM_{finer}_2%$\overline{S}$	4.71	7.96	4.35	10.67
LC^3-$CM_{coarser}$_2.5%$\overline{S}$	4.91	8.58	2.63	15.46
LC^3-CM_{finer}_2.5%$\overline{S}$	4.73	8.01	2.28	14.26
LC^3-$CM_{coarser}$_3%$\overline{S}$	4.86	8.67	1.05	20.85
LC^3-CM_{finer}_3%$\overline{S}$	4.76	7.99	1.33	27.75
LC^3-$CM_{coarser}$_3.5%$\overline{S}$	4.87	8.76	0.4	28.84
LC^3-CM_{finer}_3.5%$\overline{S}$	4.83	8.36	*	*
LC^3-$CM_{coarser}$_4%$\overline{S}$	4.98	8.23	*	12.14
LC^3-CM_{finer}_4%$\overline{S}$	4.91	7.43	*	10.38

*Approximate values

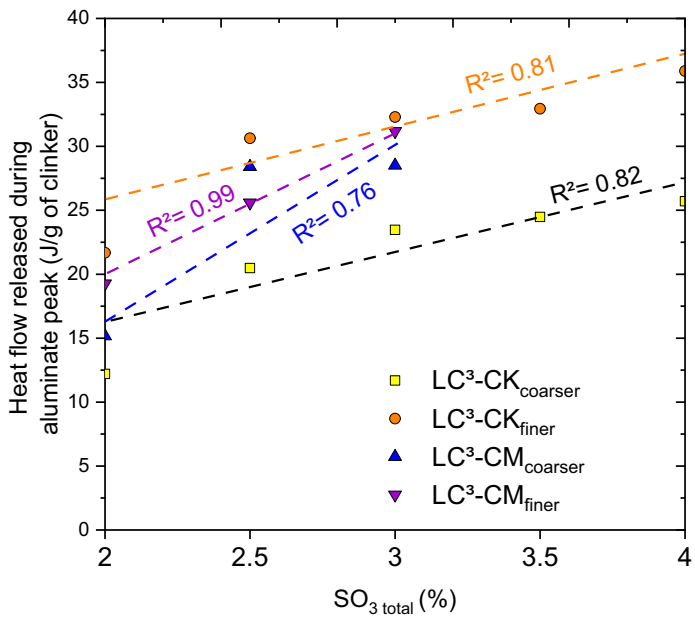

Fig. 5 Correlation between heat flow released at 72 h with SO_3 levels of LC_3 systems

between the formation of ettringite and AFm phase at 24 h with aluminate peak's intensity ($R^2 = 0.97$) from its deconvolution by super-sulfated comparison systems. From such an approach, the LC^3 aluminate peak area was also calculated concerning cement type and SO_3 content in coarser and finer LC^3-CK and -CM cements, as presented in Fig. 5. The point where the trend line intersects the y-axis suggested that the finer the calcined clay the greater its potential formation of ettringite and AFm phases, which would correspond to cements $LC^3\text{-}CK_{finer} > LC^3\text{-}CK_{coarser} > LC^3\text{-}CM_{finer} > LC^3\text{-}CM_{coarser}$.

By comparing all the cements, it was found values of heat flow released during the aluminate peak within the range observed by Zunino and Scrivener [13] in LC^3 systems with calcined kaolinite clays. In general, the higher the total SO_3 content, the larger the area of the aluminate peak, which agrees very well with the statement regarding hydration, i.e., the greater the amount of hydrated products, such as ettringite. $LC^3\text{-}CK_{coarser}$ reached numbers from ~ 12.2 to 25.7 J/g of clinker. When the CK was more finely ground, there was, on average an increase of about 44% in the results, reaching values of 21.7–35.9 J/g clinker in $LC^3\text{-}CK_{finer}$. Regarding LC^3 with CM, $LC^3\text{-}CM_{coarser}$ reaches values between 15.1 and 28.4 J/g of clinker, but when CM was finely ground, there was an increase of 58% in the results reaching values between 19.3 and 31.2 J/g of clinker in $LC^3\text{-}CM_{finer}$. The results confirm that the finer the clays, the higher the intensity of the aluminate peak, as shown by Zunino and Scrivener [13]. Furthermore, although CK is more reactive than CM, the results between the cements seem similar when analyzing clays of closer fineness, indicating a negligible impact on the chemical composition (mineralogy) of these materials.

The mechanism that dominates the intensity of that aluminate peak (whether physical or chemical) is still under discussion. Zunino and Scrivener [13] compared a LC^3 with MK 95% (kaolinite content) and $SSA_{BET} = 13.53 m^2/g$ (3% add. of gypsum) against a LC^3 with MK 50% (kaolinite content) and $SSA_{BET} = 62.61 m^2/g$ (3% add. of gypsum), concluding that the fineness of calcined clays has more impact on aluminate peak than the mineral composition. However, they compared systems under different SO_{3total} contents and without comparison for clays of the same fineness or kaolinite content. The same predominance of fineness over calcined clay chemistry was found by Py [33]. The author produced LC^3 cements with two kaolinite clays: HMK (78.25% of kaolinite clay) $SSA_{BET} = 34.4 m^2/g$, and MMK (46.1% of kaolinite clay) $SSA_{BET} = 77.5 m^2/g$. As result, all the mixes with MMK were undersulfated even its lower reactivity than HMK clay.

On the other hand, there are some studies where the clays' chemical composition, specifically the kaolinite content, had a higher impact on the sulfate demand of LC^3 [11, 19]. Malacarne et al. [34], for instance, assessing the impact of low-grade materials on LC^3 hydration, observed that higher kaolinite content, higher intensity of aluminate peak. The authors used two calcined kaolinite clays, one called natural clay (83% of kaolinite clay, NC) $SSA_{BET} = 11.8 m^2/g$, and the other as argillite (35% of kaolinite clay, AR) $SSA_{BET} = 24.7 m^2/g$. Therefore, all the previous studies have indicated that when the SSA_{BET} of calcined clays are close to each other, the chemical composition (in terms of kaolinite content) has more impact on the intensity of the aluminate peak than the fineness; on the other hand, when the comparison is made between clays with very distant SSA_{BET}, the fineness dominates the intensity of this peak, rather than kaolinite content.

The fineness of the calcined clay also impacted the cement pastes' total heat at 72 h. In the case of LC^3-CK, the finer the calcined clay, the greater the total heat at 72 h. $LC^3\text{-}CK_{coarser}$, for instance, had values between 400.1 and 431 J/g of clinker while $LC^3\text{-}CK_{finer}$ between 406.8 and 440.5 J/g of clinker. On the other hand, $LC^3\text{-}CM_{coarser}$ had values between 373.0 and 398.6 J/g of clinker, whereas $LC^3\text{-}CM_{finer}$ were 368.3–387.6/ J of clinker. This suggests that a longer grinding time reduced the CM reactivity despite the reduction of its PSD, which may occur due to the changes in the structure of the particles. In several cases, the increase in fineness of the same clay did not significantly impact the compressive strength of LC^3 pastes ($P > 0.05$, n.s.), as shown in Fig. 6.

At 3 days, the increase in fineness increased the compressive strength of almost all SO_3 contents, except for 3.5% and 2% SO_3 levels for LC-CK and -CM, respectively. The similar strength results between -CK and -CM cements (due to their close

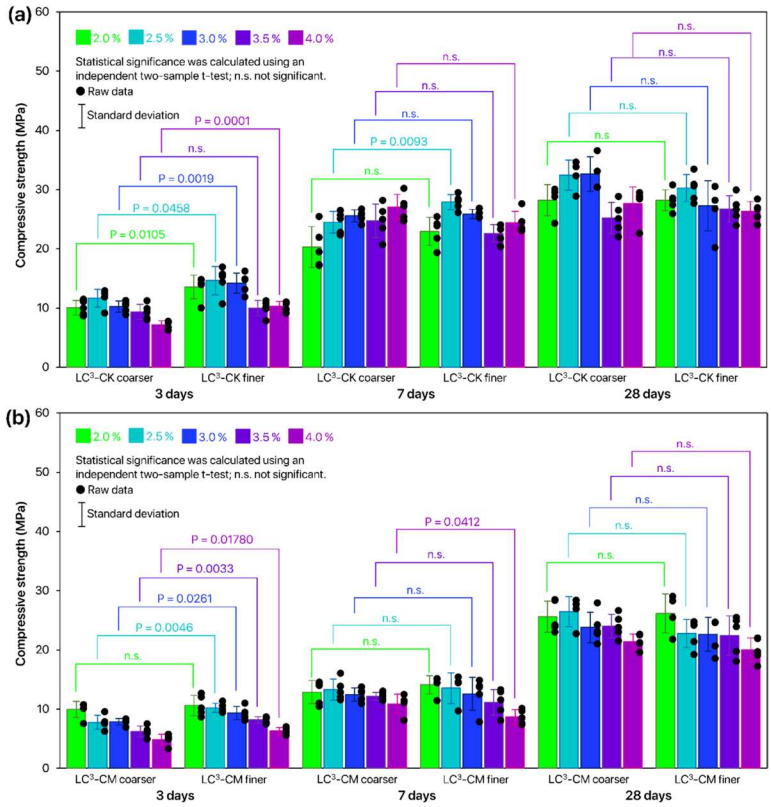

Fig. 6 Impact of calcined clay fineness on the LC^3 compressive strength of pastes with different SO_3 contents

finenesses) demonstrate how the physical effect dominates the initial hydration.

At 7 days, there was an increase in strength due to the advancement of the cement hydration reactions, which tended to be more noticeable with LC^3-CK than LC^3-CM in both finenesses. It is well-known that calcined clays, by pozzolanic reactions, interact with the products of Portland cement reactions, such as portlandite to form C–A–S–H. It is likely that the formation of Hc and Mc phases, which ongoing faster in LC^3-CK contributed to compressive strength results. Also, note that the calcined clay fineness had no significant impact on most mixes, comparing the same SO_3 content, except for 2.5% and 4.5% SO_3 levels of the cements LC^3-CK and—CM, respectively.

The most noticeable behavior (from 7 to 28 days) was the higher strength increase in LC^3-CM than in LC^3-CK, probably due to the CM pozzolanic reaction and possible porosity refinement in the case of LC^3-CK that limited higher compressive strength results. In LC^3 systems with high kaolinite content, such as CK with about 90% kaolinite content, a porosity refinement phenomenon up to a critical point where there was no more space for hydration products to be formed, as observed by Avet and Scrivener [19] when studying the impact of kaolinite content in LC^3. This porosity refinement may not have occurred with LC^3-CM due to its lower SSA BET and lower ion dissolution availability, which will be discussed further below.

3.2 Hypothesis 2: Calcined clays have a different dissolution of Si and Al ions to interact with calcium sulfate ions

The concentration of ions in the artificial pore solution (pH = 13) with CK, CM and GYP as well as their weight loss over time are shown in Fig. 7. It is worth noting that the dissolution values may not represent the real values of ions dissolution in the real pore solution during cement hydration, but the technique aims to establish a comparative parameter between the evaluated materials.

The amount of residue (%) filtered over time is shown in Fig. 10a. Due to its high dissolution under alkaline conditions, GYP showed an amount of

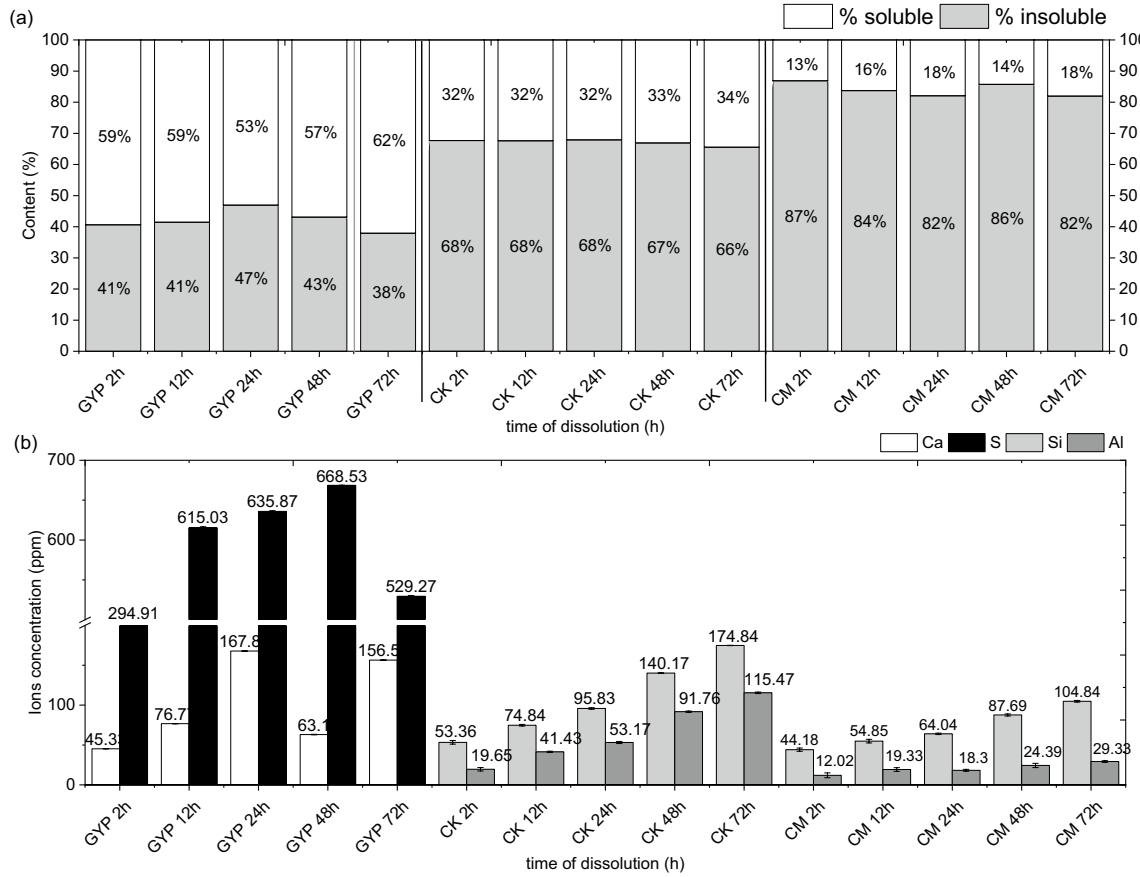

Fig. 7 Kinetics dissolution of GYP, CK_{finer} and CM_{finer} in alkaline solution

soluble material between 59 and 62%. The calcined clays had a low variation of soluble percentage with time, between 32–34% and 10–16% for the CK and CM clays, respectively. According to Scherb et al. [35], this proximity between the weighed samples is expected as it assumes that crystalline phases do not dissolve during the test, which measures the soluble part of the samples such as Ca, S, Si or Al ions.

The soluble material, then understood as ICP-OES measured the ions dissolved in the solution. The results shown in Fig. 10b reveal a progressive dissolution of Si and Al in both calcined clays over time. CK had values between 53.4–174.84 ppm of Si and 19.65–115.5 ppm of Al. Such dissolution was somewhat lower in CM, the concentration values were between 44.2–104.8 ppm of Si and 12–29.3 ppm of Al. Regarding GYP, there were the highest levels of ions dissolved in the solution. The fast and high dissolution of calcium sulfate during the cement hydration is well-known in the literature [36]. The dissolution of S ions was from 3.5 to 10.5 times higher than Ca dissolution in the mineral GYP. Also, a non-linear dissolution of Ca and S ions was observed over time. After an ascendant dissolution of Ca up to 24 h, there was a decrease in 48 h, while S ions, just happened at 72 h. The circumstances that led to these results are unclear but can suggest problems related to the saturation conditions of the solution.

Before calcination, CK is based on 1:1 mineral, with one tetrahedral layer of Si and an octahedral layer of Al, whereas CM is based on 2:1 mineral, as there is an extra Si layer covering the Al layer [37]. Despite this, neither Si nor Al ions' dissolution were higher in CM than in CK. Instead, the Si/Al ratios decreased in CK from 2.72 (2 h) to 1.51 (72 h), demonstrating the greater dissolution of Al ions in the solution. Meanwhile, CM had incongruent results related to Si/Al ratios over time, such as an increased

Si/Al at 24 h (Si/Al = 3.5) after the decrease observed from 12 h (Si/Al = 3.67) to 12 h (Si/Al = 2.84) and a decreased at 72 h (Si/Al = 3.58) after an increased from 24 h (Si/Al = 3.5) to 48 h (Si/Al = 3.59).

There are numerous reasons to explain the higher dissolution of kaolinite than montmorillonite, as discussed by Garg and Skibsted [21]. First, the lower amount of OH^- groups and the double Si layer covering Al layer from both sides greatly inhibit the hydrolysis of montmorillonite clays. Second, after efficiency calcination, calcined kaolinite clays become materials predominantly amorphous with preferential sites of Al for dissolution. ^{27}Al NMR results suggest dissolution of pentahedral coordinated Al sites (Al^V) is preferential compared to tetrahedral Al sites (Al^{IV}) [7]. Third, the incongruent dissolution and lower reactivity of montmorillonite clays can be explained by forming a passivating layer of Al^{VI} or secondary product on the surface of these clays, as evidenced by the ^{27}Al{1H} CP/MAS technique. In another study, Yokoyama et al. [38] indicated that the dissolution rate of montmorillonite depends on the outer surface rather than the total surface area in alkaline conditions, based on atomic force microscopy (AFM) analysis.

A better understanding of how the dissolution kinetics of calcined clays happen brings insights into their pozzolanic reactivity and behavior in cementitious systems, such as hydration and sulfate demand. Recently, the role of alumina (Al) content and filler effect on the sulfate requirement was discussed by Zunino and Scrivener [20]. Comparing blended cement with PC and slags (S1 and S8) of different fineness and alumina content, they observed a greater degree of reaction of alite and ettringite formation, simultaneously, a lower content of C_3A and gypsum in cements with lower alumina content (Slag 1 low Al_2O_3), but with one SSA_{BET} twice as high as the other (Slag S8 high Al_2O_3). The authors concluded that the Al content does not dominate the overall sulfate requirement in blended cements. They assumed that only the filler effect plays a role in the sulfate depletion due to its influence on C–(A)–S–H formation, and disagree with authors such as Andrade Neto et al. [18], who said that Al content might also impact the sulfate depletion. For this purpose, Zunino and Scrivener [20] reaffirmed that in the example of Avet and Scrivener [19], the silicate peaks are different (height, width, and position) between an LC^3-MK (95% kaolinite) and LC^3-MK (50% kaolinite), indicating different C–(A)–S–H contents, although heat released at the onset of the aluminate peak were similar. More recently, Zunino and Scrivener affirmed that the potential contribution of alumina from reactive SCMs like slag and metakaolin to ettringite precipitation during the acceleration phase cannot be excluded, yet its impact on sulfate requirement is limited and not directed related to the SCM's alumina content studied by them [20].

Although it is plausible the high impact of the C–(A)–S–H formation on the acceleration of the sulfate depletion, it was observed that the chemical impact (dissolution of Al) cannot be considered a factor of minor impact comparing both ternary blended cements (with CK or CM). As observed by calorimetry results all the silicate peaks (among all SO_3 contents) were quite similar (height, width, and position) between CK and CM systems, although their different SSA_{BET}. The main differences were observed in the aluminate peak, where the second precipitation of ettringite intensified because Al ions were released into the pore solution, as the ICP-OES comparison suggests. Also, with the rapid and high dissolution of gypsum into SO_4^{2-} (higher than Ca^{+2}) more ions were available to interact with Al, for instance, higher in CK than CM.

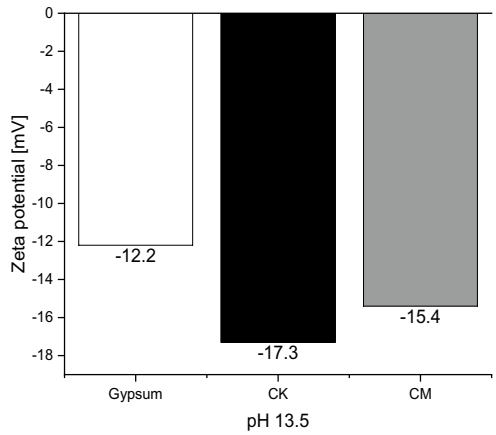

Fig. 8 Zeta potential of GYP, CK_{finer} and CM_{finer} in the artificial pore solution

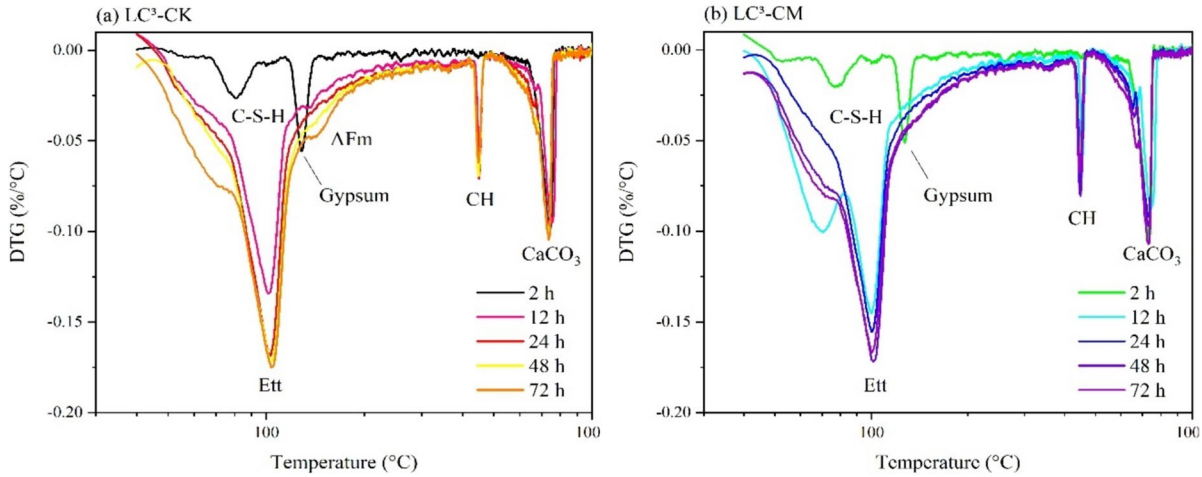

Fig. 9 DTG curves of **a** LC^3-CK and **b** LC^3-CM pastes at 2, 12, 24, 48 and 72 h

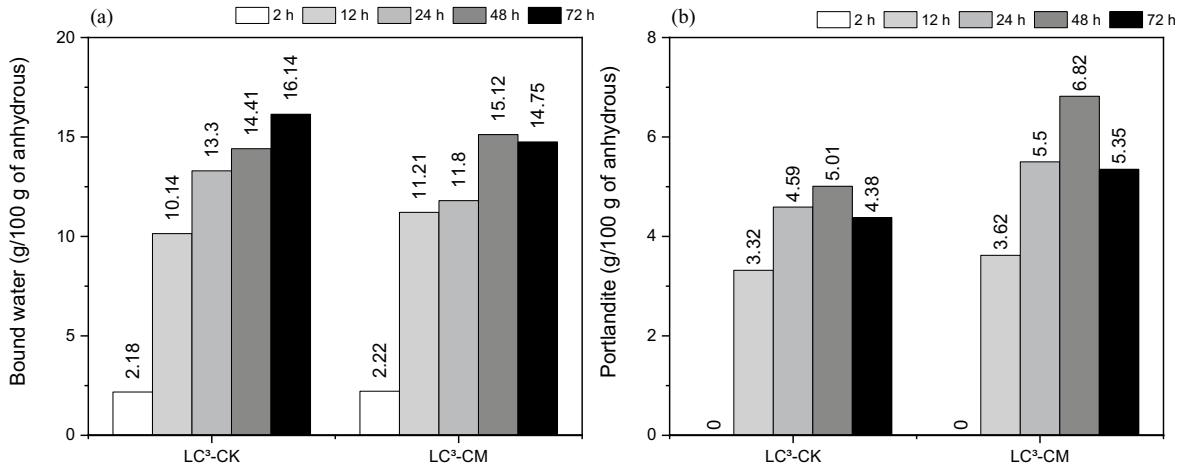

Fig. 10 **a** Bound water and **b** Portlandite content of LC^3 pastes at different ages

3.3 Hypothesis 3: calcined clays have a different capacity to adsorb ions from calcium sulfate

Another aspect that may influence the kinetics of hydration and sulfate depletion is the possible adsorption that calcium sulfate ions may have on the surface of the calcined clays. As observed in Fig. 8, the zeta potential values of GYP, CK, and CM in an artificial pore solution (pH = 13.5) were − 12.2, − 17.3 and − 15.4 mV, respectively.

Throughout the hydration of LC^3, there are interactions between the surface of calcined clays and gypsum. However, it is unclear to what extent these interactions can drive the sulfate balance. As known, after the contact of cement with water, clinker phases, such as C_3A, rapidly dissolve to form the first crystals of ettringite in contact with gypsum Myers et al. [39]. Based on zeta potential results, Maier et al. [14] found that the adsorption of SO_4 and/or Ca-SO_4 complexes from gypsum onto calcined clay surface was the main factor inhibiting C_3A hydration in the absence of silicate reactions. However, the impact of the charges provided by calcined clays as the main impact on the sulfate depletion of LC^3 is not fully understood.

First, the fact of the calcium sulfate being adsorbed to C–S–H until its depletion point is considered by

Zunino and Scrivener [20] as the main factor reducing the availability of gypsum in solution, which could explain the fast sulfate depletion in LC^3 systems. More testes need to be performed to confirm the calcium sulfate's preferential and higher adsorption on C–(A)–S–H than on the surface of the calcined clays. If we look at the dissolution results (Fig. 10), simultaneously, the gypsum released more S ions, which in solution would be sulfur (S) ions complexes, than Ca cations (in the form of Ca^{+2}), explaining the negative zeta potential results of the GYP.

On the other side are the calcined clays (CK and CM). They release Si cations and Al ions (Al_2O_3) into a pore solution containing alkalis from the clinker. The resulting charge balances in the zeta plane suggest that the calcined clays are negative and, among other ions, will preferably interact with Ca ions, when it happens, the pore solution of systems with clays will become gradually positively charged. Lei and Plank [22] proved an increasing and positive alteration of zeta potential results as a function of Ca^{+2} additions into alkaline solution with different phyllosilicates such as muscovite, kaolinite and montmorillonite, which would illustrate the affinity of (surface) calcined clay for Ca ions, such as from, gypsum, etc. Also, the ability of the clay surfaces to interact with Ca^{+2} ions was measured by gradually dripping a solution of $CaCl_2.2H_2O$, based on that described by Schmid and Plank [40]. The results indicated that the more negative the zeta potential, the greater the ability of the solution material to interact with Ca^{2+} ions. Thus, such adsorption may happen higher in CK than CM, due to its negative charge of slightly greater magnitude. Given this discussion, it is likely that the adsorption of calcium sulfate ions has less impact than its adsorption on C–(A)–S–H surfaces but more studies are needed.

3.4 Early-age hydration of limestone calcined clays cements

Figure 9 shows the DTG curves of the LC^3-CK_{finer} and LC^3-CM_{finer} pastes at 2, 12, 24, 48 and 72 h with 2.5% SO_{3total} Peaks related to the evaporation of free water (below 100 °C), decomposition of ettringite (at ~ 110 °C), gypsum (at ~ 120 °C), AFm phases (at ~ 150 °C), C–S–H (50 to 600 °C), portlandite (between 400 and 500 °C) and calcium carbonates from the limestone (between 650 and 800 °C) [28] are observed.

One can note that at 2 h there was still gypsum in both samples, while at 12 h there was no evidence of gypsum, indicating that the sulfate depletion already occurred. At 2 h, the DTG data for both cements did not show evidence of the presence of portlandite, indicating a limited alite hydration up to this period, which agrees with calorimetry results (both pastes still were in the induction period at 2 h), and with previous studies [41, 42]. From 12 h, it was observed ettringite, C–S–H and portlandite DTG peaks for both pastes, as expected. Finally, at 72 h was it possible to see AFm peak for the LC^3-CK paste, while the LC^3-CM did not present a distinguished AFm peak. This evidences that the CK clay promotes an earlier formation of AFm phases when compared to the CM clay, which can be related to the higher reactivity (Fig. 2) and Al solubility of the CK clay as shown in Fig. 7. As observed by De Matos et al. [41], when studying calcined kaolinites clays with different amorphous/kaolinite content, the LC^3 cements with the clay with 97.62% of ACn (Amorphous and Crystalline non-quantified) content resulted in ~12 h earlier hemicarbonate formation than the cements with a clay with 91.11% of ACn. The earlier AFm formation in the LC^3 with high reactivity kaolinite clays was also observed by some authors [43, 44].

The bound water and portlandite contents of the LC^3 pastes are presented in Fig. 10. With the progress of the hydration, the bound water content increases, as expected. Comparing both cements, no significant differences in the bound water content were observed (Fig. 8a), which agrees with the calorimetry results (see Fig. 4, where both cements present similar cumulative heat curves). Regarding the portlandite content (Fig. 8b), the pastes showed similar contents up to 12 h. However, after 24 h, the LC^3-CK paste presented lower portlandite contents than the LC^3-CM paste. This might indicate a very early pozzolanic activity from the LC^3-CK, which agrees with previous studies [41, 43, 44]. After 48 h, one can note a decrease in portlandite content in the LC^3-CM paste, indicating an early pozzolanic activity of CM clay as well.

Figure 11 presents selected ranges of the XRD patterns (7–13 and 16–20°2θ) of LC^3-CK (a, b) and LC^3-CM (c, d) pastes at 2, 12, 24, 48 and 72 h. For both cements, at 2 h gypsum ($CaSO_4.2H_2O$; ICSD

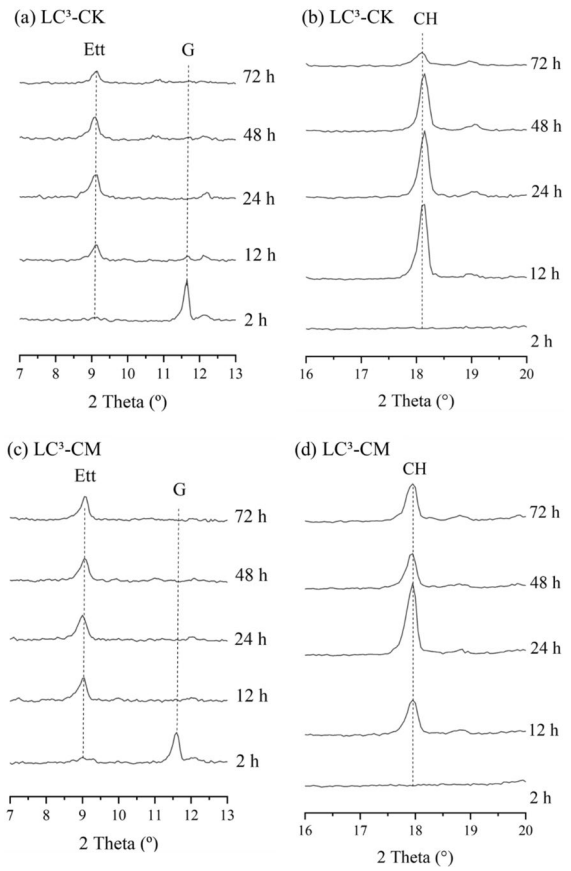

Fig. 11 XRD patterns of LC^3-CK (**a, b**) and LC^3-CM (**c, d**) hydrated pastes. *Ett* Ettringite, *G* Gypsum, *CH* Portlandite

409581) was still present, while no XRD peaks of ettringite ($Ca_6Al_2(SO_4)_3(OH)_{12}{\cdot}_{26}H_2O$; ICSD 155395) and portlandite (Ca (OH) $_2$; ICSD 202220) were observed. In turn, at 12 h, the gypsum XRD peak was not present anymore, indicating that sulfate depletion already occurred for both cements. This agrees with calorimetry and TGA results, as previously discussed. At 12 h, ettringite and portlandite peaks were present and remain for the rest of the time tested. Finally, despite the LC^3-CK paste presenting AFm DTG peaks at 72 h, no AFm peaks were observed in the XRD, probably due to the poorly crystallinity nature of the AFm-type phases [45, 46].

4 Conclusion

This study investigated the effects of two calcined clays with different mineralogy (kaolinite and montmorillonite) on the hydration of blended cements. The impact of these clays on sulfate depletion kinetics was investigated from the point of view of three hypotheses: (1) impact of fineness, (2) dissolution of Si and Al ions, and (3) possible adsorption of calcium sulfate ions into calcined clay's surface. The main results were:

- *Impact of fineness* the analyzed fineness of the clays in this study had minor influence on the results of compressive strength and hydration kinetics. Therefore, it was not the mechanism that dominated the accelerated sulfate depletion when comparing CK with CM clays.
- *Dissolution of S and Al ions* the chemical effect that clays have on the sulfate balance was the main explanation found when comparing clays of close fineness but different mineralogy. The higher dissolution of ions (especially Al) from the CK increases the intensity of the aluminate peaks and accelerates the sulfate depletion by competing ions to form ettringite.
- *Adsorption of calcium sulfate ions into calcined clay's surface* the negative zeta potential values of the calcined clays in solution demonstrate their affinity for interaction with Ca^{2+} ions (either from gypsum or from clinker), but the results cannot confirm it as the main mechanism driving the sulfate balance of the LC^3. The adsorption of sulfate ions on C–S–H can be a justification but it needs to be further investigated.

These results provide new insight into the mechanisms involved in the sulfate balancing of LC^3s, comparing kaolinite with montmorillonite clays. Here we demonstrated that the chemical effect of the clays has the most significant impact on achieving the correct sulfate balance, and that alternative clays to metakaolin, such as bentonites (rich in montmorillonites) can be an alternative to minimize the problem of accelerated sulfate depletion in LC^3 mixes.

Acknowledgements Intercement Participações S.A. supported the participation of MRCS. The participation of JSAN was supported by the fellowship DAI/CNPq (National Council of Scientific and Technological Development–Brazil)/Intercement. The participation of BW was sponsored by The Department of Chemical and Biological Engineering, The University of Sheffield. CNPq sponsored APK through the research fellowship 311893/2021-0. This work is part of the research project UNIVERSAL Grant Number 427958/2018-0. The authors would like to thank the cement industry for the materials supplied and Maurilio Gomes-Pimentel for the statistical analysis.

Declarations

Conflict of interest The authors declare that they have no known competing financial interests or personal relationships that could have appeared to influence the work reported in this paper.

References

1. Ito A, Wagai R (2017) Global distribution of clay-size minerals on land surface for biogeochemical and climatological studies. Sci Data 4:1–11. https://doi.org/10.1038/sdata.2017.103
2. Garg N (2015) Structure, reactivity, and dissolution of calcined clays by solid-state NMR. Aarhus University, New York
3. Ma Y, Shi C, Lei L et al (2020) Research progress on polycarboxylate based superplasticizers with tolerance to clays—a review. Constr Build Mater 255:119386
4. Mandalia T, Bergaya F (2006) Organo clay mineral–melted polyolefin nanocomposites effect of surfactant/CEC ratio. J Phys Chem Solids 67:836–845. https://doi.org/10.1016/J.JPCS.2005.12.007
5. Murray HH (2006) Chapter 6 Bentonite applications. In: Developments in clay science, pp 111–130
6. Flegar M, Serdar M, Londono-Zuluaga D, Scrivener K (2019) Overview of clay as supplementary cementitious material. Simp DOKTORSKOG Stud GRAĐEVINARSTVA. https://doi.org/10.5592/CO/PhDSym.2019.14
7. Fernandez R, Martirena F, Scrivener KL (2011) The origin of the pozzolanic activity of calcined clay minerals: a comparison between kaolinite, illite and montmorillonite. Cem Concr Res 41:113–122. https://doi.org/10.1016/j.cemconres.2010.09.013
8. Antoni M, Rossen J, Martirena F, Scrivener K (2012) Cement substitution by a combination of metakaolin and limestone. Cem Concr Res 42:1579–1589. https://doi.org/10.1016/j.cemconres.2012.09.006
9. Cementir Holding (2020) The cement of the future is now here: cementir launches FUTURECEM^{TM} with up to 30 percent lower carbon emissions. Cementir Holding N.V. https://www.cementirholding.com/en/media/whats-new/cement-future-now-here-cementir-launches-futurecemtm-30-percent-lower-carbon. Accessed 10 Jun 2021
10. Juenger MCG, Snellings R, Bernal SA (2019) Supplementary cementitious materials: new sources, characterization, and performance insights. Cem Concr Res 122:257–273
11. da Silva MRC, Malacarne CS, Longhi MA, Kirchheim AP (2021) Valorization of kaolin mining waste from the Amazon region (Brazil) for the low-carbon cement production. Case Stud Constr Mater 15:e00756. https://doi.org/10.1016/J.CSCM.2021.E00756
12. Scrivener AF, Maraghechi H et al (2019) Impacting factors and properties of limestone calcined clay cements (LC 3). Green Mater 7:3–14. https://doi.org/10.1680/jgrma.18.00029
13. Zunino F, Scrivener K (2019) The influence of the filler effect on the sulfate requirement of blended cements. Cem Concr Res. https://doi.org/10.1016/j.cemconres.2019.105918
14. Maier M, Scherb S, Neißer-Deiters A et al (2021) Hydration of cubic tricalcium aluminate in the presence of calcined clays. J Am Ceram Soc 104:3619–3631. https://doi.org/10.1111/jace.17745
15. Taylor-Lange SC, Lamon EL, Riding KA, Juenger MCG (2015) Calcined kaolinite-bentonite clay blends as supplementary cementitious materials. Appl Clay Sci 108:84–93. https://doi.org/10.1016/j.clay.2015.01.025
16. Wei J, Gencturk B (2019) Hydration of ternary Portland cement blends containing metakaolin and sodium bentonite. Cem Concr Res. https://doi.org/10.1016/j.cemconres.2019.05.017
17. Shi Z, Ferreiro S, Lothenbach B et al (2019) Sulfate resistance of calcined clay-Limestone-Portland cements. Cem Concr Res 116:238–251. https://doi.org/10.1016/j.cemconres.2018.11.003
18. da Andrade Neto JS, De Torre AG, Kirchheim AP (2021) Effects of sulfates on the hydration of Portland cement—a review. Constr Build Mater. https://doi.org/10.1016/j.conbuildmat.2021.122428
19. Avet F, Scrivener K (2018) Investigation of the calcined kaolinite content on the hydration of Limestone Calcined Clay Cement (LC3). Cem Concr Res 107:124–135. https://doi.org/10.1016/j.cemconres.2018.02.016
20. Zunino F, Scrivener K (2022) Insights on the role of alumina content and the filler effect on the sulfate requirement of PC and blended cements. Cem Concr Res 160:106929. https://doi.org/10.1016/j.cemconres.2022.106929

21. Garg N, Skibsted J (2019) Dissolution kinetics of calcined kaolinite and montmorillonite in alkaline conditions: evidence for reactive Al(V) sites. J Am Ceram Soc 102:7720–7734. https://doi.org/10.1111/JACE.16663
22. Lei L, Plank J (2014) A study on the impact of different clay minerals on the dispersing force of conventional and modified vinyl ether based polycarboxylate superplasticizers. https://doi.org/10.1016/j.cemconres.2014.02.009
23. Avet F, Snellings R, Alujas Diaz A et al (2016) Development of a new rapid, relevant and reliable (R^3) test method to evaluate the pozzolanic reactivity of calcined kaolinitic clays. Cem Concr Res 85:1–11. https://doi.org/10.1016/j.cemconres.2016.02.015
24. Momma K, Izumi F (2011) VESTA 3 for three-dimensional visualization of crystal, volumetric and morphology data. J Appl Crystallogr 44:1272–1276. https://doi.org/10.1107/S0021889811038970
25. ABNT (2018) NBR 16697: Cimento Portland-Requisitos
26. ASTM (2018) C563:18—standard guide for approximation of optimum SO_3 in hydraulic cement 1. https://doi.org/10.1520/C0563-19
27. Snellings R, Chwast J, Cizer Ö et al (2018) RILEM TC-238 SCM recommendation on hydration stoppage by solvent exchange for the study of hydrate assemblages. Mater Struct Constr 51:1–4. https://doi.org/10.1617/S11527-018-1298-5/METRICS
28. Lothenbach B, Durdzinski PT, de Weerdt K (2016) Thermogravimetric analysis. In: Scrivener K, Snellings R, Lothenbach B (eds) A practical guide to microstructural analysis of cementitious materials. CCR Press, pp 177–212
29. Beuntner N, Thienel C, Beuntner N, Thienel K-C (2016) Solubility and kinetics of calcined clay: study of interaction by pore solution
30. Scherb S, Maier M, Beuntner N et al (2021) Reaction kinetics during early hydration of calcined phyllosilicates in clinker-free model systems. Cem Concr Res 143:106382. https://doi.org/10.1016/J.CEMCONRES.2021.106382
31. Berodier E, Scrivener K (2014) Understanding the filler effect on the nucleation and growth of C-S-H. J Am Ceram Soc 97:3764–3773. https://doi.org/10.1111/JACE.13177
32. Baki VA, Ke X, Heath A et al (2022) The impact of mechanochemical activation on the physicochemical properties and pozzolanic reactivity of kaolinite, muscovite and montmorillonite. Cem Concr Res. https://doi.org/10.1016/J.CEMCONRES.2022.106962
33. Py LG (2021) Balanceamento de sulfatos e hidratação de cimentos ternários à base de calcários e argilas calcinadas. Universidade Federal do Rio Grande do Sul
34. Malacarne C, Longhi MA, Silva MRC et al (2021) Influence of low-grade materials as clinker substitute on the rheological behavior, hydration and mechanical performance of ternary cements. Case Stud Constr Mater 15:e00776. https://doi.org/10.1016/J.CSCM.2021.E00776
35. Scherb S, Köberl M, Beuntner N et al (2020) Reactivity of metakaolin in alkaline environment: correlation of results from dissolution experiments with XRD quantifications. Materials (Basel). https://doi.org/10.3390/ma13102214
36. Tang FJ, Gartner EM (1988) Influence of sulphate source on Portland cement hydration. Adv Cem Res 1:67–74. https://doi.org/10.1680/adcr.1988.1.2.67
37. Bergaya F, Lagaly G (2013) General introduction: clays, clay minerals, and clay science. Dev Clay Sci 5:1–19. https://doi.org/10.1016/B978-0-08-098258-8.00001-8
38. Yokoyama S, Kuroda M, Sato T (2005) Atomic force microscopy study of montmorillonite dissolution under highly alkaline conditions. Clays Clay Miner 532(53):147–154. https://doi.org/10.1346/CCMN.2005.0530204
39. Myers RJ, Geng G, Li J et al (2016) Role of adsorption phenomena in cubic tricalcium aluminate dissolution. https://doi.org/10.1021/acs.langmuir.6b03474
40. Schmid M, Plank J (2021) Interaction of individual meta clays with polycarboxylate (PCE) superplasticizers in cement investigated via dispersion, zeta potential and sorption measurements. Appl Clay Sci 207:106092. https://doi.org/10.1016/J.CLAY.2021.106092
41. de Matos PR, Andrade Neto JS, Sakata RS et al (2022) Effect of superplasticizer addition time and metakaolin source on the early-age hydration of limestone calcined clay cement (LC3). Mater Struct. https://doi.org/10.1617/s11527-022-02049-w
42. Jansen D, Naber C, Ectors D et al (2018) The early hydration of OPC investigated by in-situ XRD, heat flow calorimetry, pore water analysis and 1H NMR: learning about adsorbed ions from a complete mass balance approach. Cem Concr Res 109:230–242. https://doi.org/10.1016/j.cemconres.2018.04.017
43. Zunino F, Scrivener K (2021) The reaction between metakaolin and limestone and its effect in porosity refinement and mechanical properties. Cem Concr Res. https://doi.org/10.1016/j.cemconres.2020.106307
44. Maier M, Sposito R, Beuntner N, Thienel K-C (2022) Particle characteristics of calcined clays and limestone and their impact on early hydration and sulfate demand of blended cement. Cem Concr Res 154:106736. https://doi.org/10.1016/j.cemconres.2022.106736
45. Andrade Neto JS, de Matos PR, De la Torre AG et al (2022) The role of sodium and sulfate sources on the rheology and hydration of C3A polymorphs. Cem Concr Res. https://doi.org/10.1016/j.cemconres.2021.106639
46. Ectors D (2016) Advances in the analysis of cementitious reactions and hydrate phases-Fortschritte in der Analyse von zementären Reaktionen und Hydratphasen